

## ATLAS Measurements of Boosted Objects

Christoph Anders  
on behalf of the  
ATLAS collaboration

Physikalisches Institut – Universität Heidelberg



August 19<sup>th</sup> 2014



Understanding behavior of “basic” boosted objects,  $W/Z$  and top, at high  $p_T$  is essential for many measurements and searches!

New or updated ATLAS cross section results since BOOST '13:

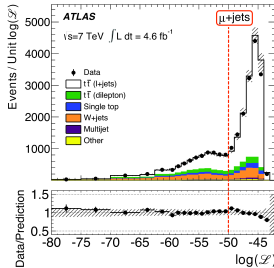
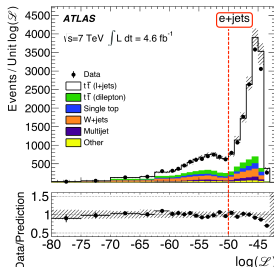
- Differential  $t\bar{t}$  cross section (July '14)
- High  $p_T$   $Z \rightarrow b\bar{b}$  cross section (April '14)
- High  $p_T$   $W/Z$  cross section (July '14)

# Differential $t\bar{t}$ Cross Section Measurements

arXiv:1407.0371 [hep-ex], submitted to PRD

3/20

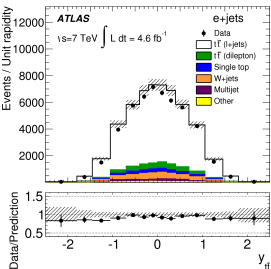
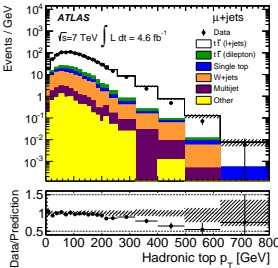
- Data:  $\sqrt{s} = 7$  TeV,  $L_{int} = 4.6 \text{ fb}^{-1}$
- Event selection:
  - Single lepton trigger
  - $1 e \text{ or } \mu, p_T > 25 \text{ GeV}, |\eta| < 2.5$
  - $\geq 4 \text{ anti-}k_t, R = 0.4$  jets,  $p_T > 25 \text{ GeV}, |\eta| < 2.5$
  - $\geq 1 \text{ b-tag}$ , MVA tagger,  $\epsilon = 70\%$
  - $E_T^{\text{miss}} > 30 \text{ GeV}$  and  $m_T^W > 35 \text{ GeV}$
- Reconstruct  $t\bar{t}$  kinematics with Likelihood fitter
- Signal MC: ALPGEN+HERWIG, CTEQ6L1
- $W+\text{jets}$  normalization and multi-jet backgrounds derived from data
- $W+\text{jets}$  shape and other bkggs from MC



# Differential $t\bar{t}$ Cross Section Measurements – II

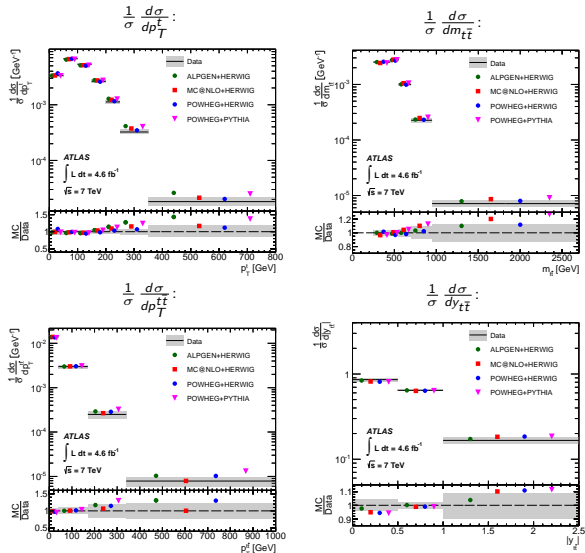
4/20

arXiv:1407.0371 [hep-ex], submitted to PRD



- Unfold data to parton-level kinematics
- Regularized Singular Value Decomposition method
- Migration matrices from  $t\bar{t}$  MC (LO)
- Main systematic uncertainties:
  - $p_T^t, m_{t\bar{t}}$ : JES (1-4%), MC gen. (1-8%), b-tagging eff. (1-4%)
  - $p_T^{t\bar{t}}$ : ISR/FSR (1-10%), MC gen. (1-9%), frag. (1-7%), JER (3-8%)
  - $y_{t\bar{t}}$ : MC gen. (1-6%), fragmentation (1-4%),
- Combine  $e$  and  $\mu$  channels with BLUE method
- Compute  $\frac{1}{\sigma} \frac{d\sigma}{dX}$ , with X:
  - $p_T^t$  (sensitive to higher order corrections @ high  $p_T$ )
  - $m_{t\bar{t}}$  (important for  $t\bar{t}$  resonance searches)
  - $p_T^{t\bar{t}}$  (sensitive to extra radiation)
  - $y_{t\bar{t}}$  (test of PDFs)
- Compare to various generators and calculations

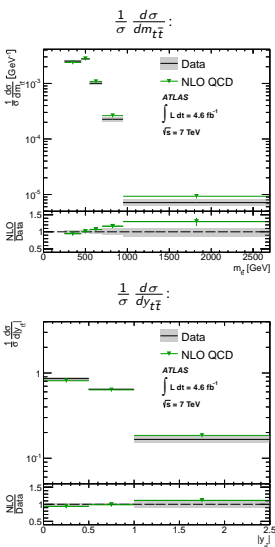
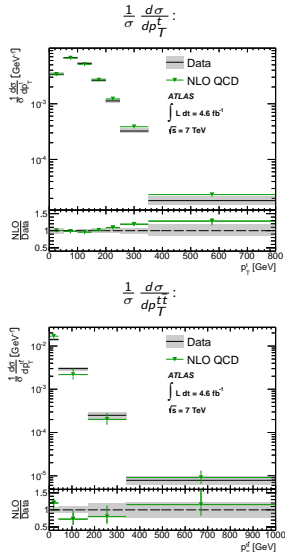
# Comparison of Unfolded Data and Different Generators 5/20



- $p_T^t$  softer in data above 200 GeV.
- No single generator performs best for all kinematic variables considered.
- $\chi^2$  tests show that the data have sufficient precision to probe the predictions!

# Comparison of Unfolded Data and NLO QCD Calculations

6/20



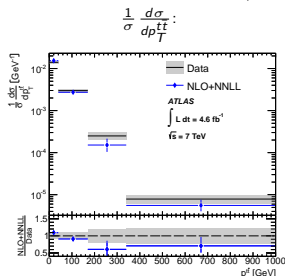
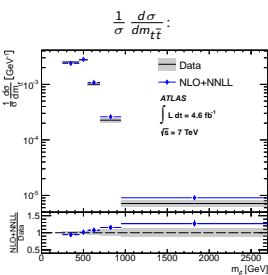
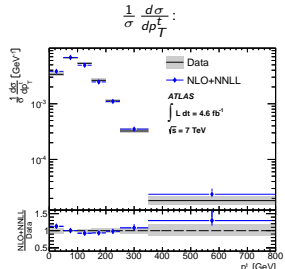
- In data  $p_T^t$  and  $m_{t\bar{t}}$  softer in tails

Details:

- QCD calculations at NLO (MCFM with CT10 PDF)
- $\mu_F = \mu_R = m_{top}$ , varied by  $\frac{1}{2}$  and 2
- CT10 PDF 68% CL error-sets

# Comparison of Unfolded Data and NLO+NNLL QCD Calculations

7/20



- In data  $p_T^t$  and  $m_{t\bar{t}}$  softer in tails

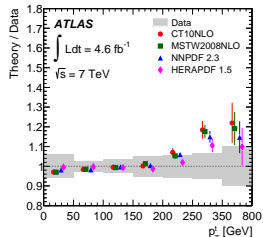
## Details:

- QCD calculations at NLO+NNLL (MSTW2008NNLO)
- Dynamic scale  $m_{t\bar{t}}$ , varied by  $\frac{1}{2}$  and 2
- PDF uncertainties for  $m_{t\bar{t}}$  and  $p_T^{t\bar{t}}$
- For  $p_T^t$  dynamic scale uncertainty  $\mu = \sqrt{m_t^2 + P_T^t}$  included

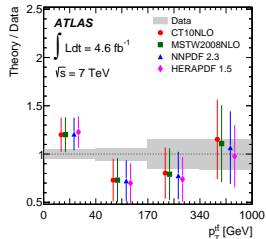
# Comparison of Unfolded Data and different PDFs

8/20

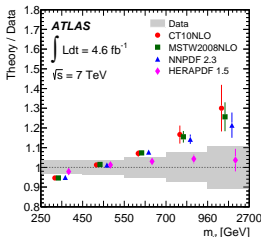
$$\frac{1}{\sigma} \frac{d\sigma}{dp_T^t} :$$



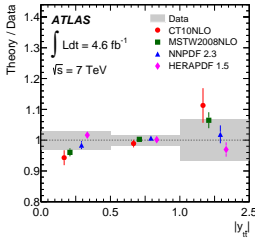
$$\frac{1}{\sigma} \frac{d\sigma}{dp_T^{t\bar{t}}} :$$



$$\frac{1}{\sigma} \frac{d\sigma}{dm_{t\bar{t}}} :$$



$$\frac{1}{\sigma} \frac{d\sigma}{dy_{t\bar{t}}} :$$

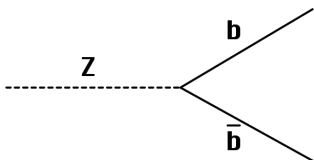


- MCFM predictions with 4 PDF sets
- Some tension at high  $p_T^t$  and  $m_{t\bar{t}}$
- Data might be usable to improve future PDF fits

# High $p_T$ $Z \rightarrow b\bar{b}$ cross section measurement

arXiv:1404.7042 [hep-ex], submitted to Physics Letters B

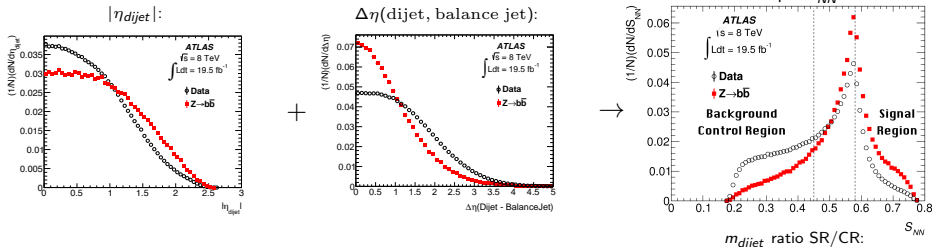
9/20



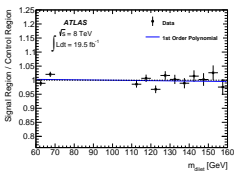
- Data:  $\sqrt{s} = 8$  TeV,  $L_{int} = 19.5 \text{ fb}^{-1}$
- Signal simulation: SHERPA
- Multi-jet background: from data
- Other small backgrounds from simulation.
- OR of six jet based triggers.
- $3 \leq n_{jet} \leq 5$ :  
anti- $k_t$   $R = 0.4$ ,  $p_T > 30$  GeV,  $|\eta| < 2.5$
- $n_{b-jet} = 2$ :  
MVA,  $\epsilon = 70\%$ ,  $p_T > 40$  GeV,  $\Delta R_{bb} < 1.2$
- Di-jet system:  
 $p_T^{dijet} = p_T^{bb} > 200$  GeV  
 $60 < m_{dijet} < 160$  GeV

# Separation from Multi-Jet Background – Neural Network

10/20



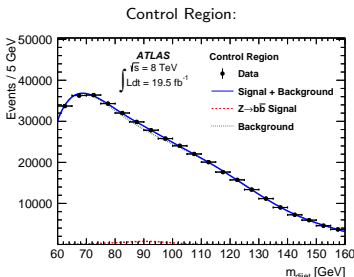
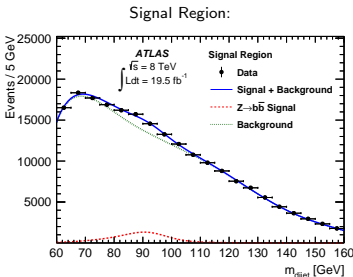
- $Z + \text{jet}$  system tends to be more boosted along beam axis than than multi-jet background.
- Use  $\eta_{dijet}$  and  $\Delta\eta(\text{dijet, balance jet})$  in NN.
- Use NN output  $S_{NN}$  to split sample in signal and control region:
  - $N_{SR}^{\text{data}} \approx 236k$ ,  $N_{CR}^{\text{data}} \approx 475k$
  - $(S/B)^{SR} = 6\%$ ,  $(S/B)^{CR} = 2\%$   
for  $m_{dijet}$  in  $[m_W - 15\text{ GeV}, m_W + 15\text{ GeV}]$



Very small correlation between NN  
and  $m_{dijet}$ !

# Signal Extraction

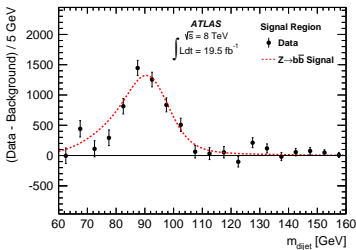
11/20



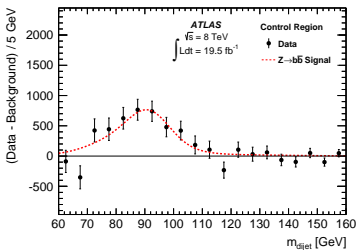
- Fit:  $m_{\text{dijet}}(60 \text{ GeV}, 160 \text{ GeV})$
- Simultaneous fit in SR and CR (binned (1 GeV), extended maximum-likelihood).
- Signal model: 3 Gaussians, yield in SR, peak position are free, other parameters fixed to MC.
- $R_Z = N_{Z \rightarrow b\bar{b}}^{CR}/N_{Z \rightarrow b\bar{b}}^{SR} = 0.62$  fixed.
- Multi-jet background: 7<sup>th</sup> order Bernstein polynomial
- Other smaller backgrounds from MC.
- Yield:  $N_{Z \rightarrow b\bar{b}} = 6420 \pm 640$  (stat.)

# Signal Extraction

Signal Region:



Control Region:



- Fit:  $m_{dijet}(60 \text{ GeV}, 160 \text{ GeV})$
- Simultaneous fit in SR and CR (binned (1 GeV), extended maximum-likelihood).
- Signal model: 3 Gaussians, yield in SR, peak position are free, other parameters fixed to MC.
- $R_Z = N_{Z \rightarrow b\bar{b}}^{CR}/N_{Z \rightarrow b\bar{b}}^{SR} = 0.62$  fixed.
- Multi-jet background: 7<sup>th</sup> order Bernstein polynomial
- Other smaller backgrounds from MC.
- Yield:  $N_{Z \rightarrow b\bar{b}} = 6420 \pm 640$  (stat.)

# Resulting Cross Section $\sigma_{Z \rightarrow b\bar{b}}$

12/20

## Measurement:

$$\sigma_{Z \rightarrow b\bar{b}}(\text{fiducial}) =$$

 $2.02 \pm 0.20 \text{ (stat.)} \pm 0.25 \text{ (syst.)} \pm 0.06 \text{ (lumi.) pb}$ 

## NLO Predictions:

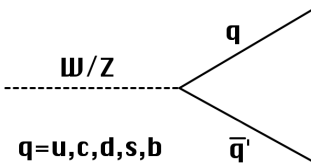
$$\sigma_{POWHEG} = 2.02^{+0.25}_{-0.19} \text{ (scales)} {}^{+0.03}_{-0.04} \text{ (PDF) pb}$$

$$\sigma_{aMC@NLO} = 1.98^{+0.16}_{-0.08} \text{ (scales)} \pm 0.03 \text{ (PDF) pb}$$

## Systematics:

Source of uncertainty	$\Delta\sigma_{Z \rightarrow b\bar{b}}^{\text{fid}}(\%)$
Jet energy scale	+6.5 / -5.0
Jet energy resolution	$\pm 5.1$
b-tagging	$\pm 3.6$
Trigger modelling	$\pm 6$
Control Region bias	+4.9 / -5.5
Signal $S_{NN}$ modelling	$\pm 2.9$
Signal $m_{\text{dijet}}$ shape	$\pm 2.2$
$Z \rightarrow c\bar{c}$ normalisation	$\pm 0.4$
$t\bar{t}$ normalisation	$\pm 1.1$
$W \rightarrow q\bar{q}'$ normalisation	$\pm 1.0$

Very good agreement!



- Data:  $\sqrt{s} = 7$  TeV,  $L_{int} = 4.6 \text{ fb}^{-1}$
- Signal MC: HERWIG+JIMMY  
scaled to NLO MCFM prediction ( $k = 1.25$ ).
- QCD jet MC: PYTHIA
- + variations for crosschecks/systematics.

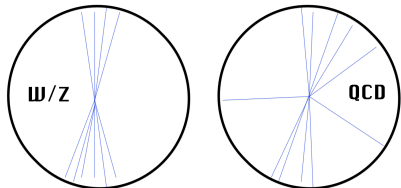
- Reconstruct  $W/Z$  in one anti- $k_t$   $R = 0.6$  jet, with  $p_T > 320 \text{ GeV}$ ,  $|\eta| < 1.9$ ,  $50 \text{ GeV} < m_{jet} < 140 \text{ GeV}$
- Limited jet mass resolution → measure
$$\sigma_{W+Z} = \sigma_W (p_T > 320, |\eta| < 1.9) \times B(W \rightarrow q\bar{q}) + \sigma_Z (p_T > 320, |\eta| < 1.9) \times B(Z \rightarrow q\bar{q})$$
- Use  $W/Z$  enriched jet sample to study several grooming methods.

# $W/Z$ Jet- QCD Jet Discrimination

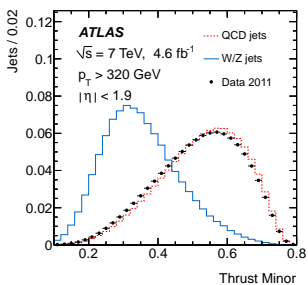
14/20

- Boost jet to its center-of-mass frame:
  - $W/Z$ : back-to-back
  - QCD: isotropic
- Analyse “jet-shapes”:

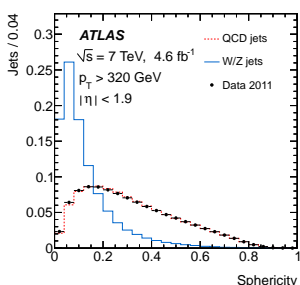
Jet center-of-mass frame:



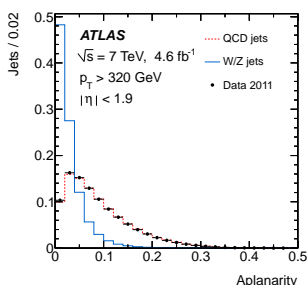
Thrust Minor:



Sphericity:

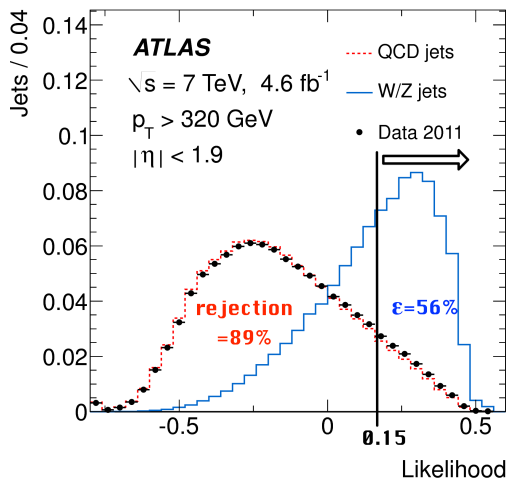


Aplanarity:



# Likelihood Discriminant

15/20

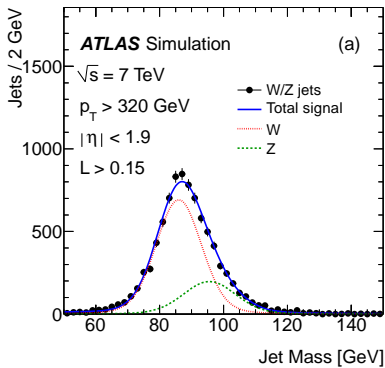


- Maximise  $S/\sqrt{S+B}$   
 $\rightarrow L > 0.15$
- Final sample:  
 $\approx 591\text{k}$  jets
- $n_{jet} > 1$  for 2.5% of selected data events

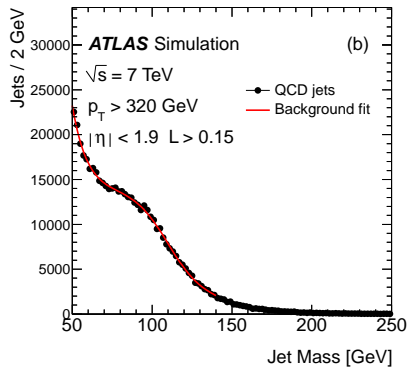
# Signal and Background Modeling

16/20

Signal:



Background:

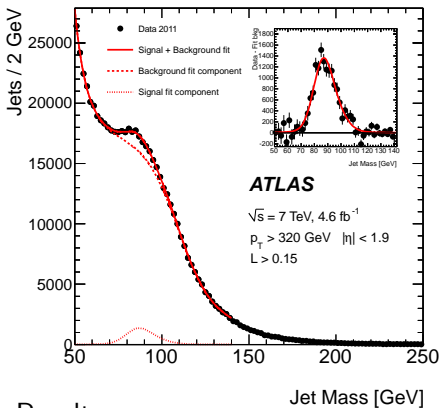


- For each  $W$  and  $Z$ :  
1 Breit-Wigner  $\otimes$  1 Gauss
- Floating:  $W/Z$  rate
- Other parameters: fixed to MC

- 2 exp. decay functions + 1 sigmoid
- $$S(\bar{m}) = \bar{m} / \sqrt{1 + \bar{m}^2} \text{ with } \bar{m} = (m_{jet} - m_0) / \sigma_m$$
- Shoulder due to selection, etc., well reproduced by QCD jet MC

# Signal Extraction and Results

17/20



Result:

$$\sigma_{W+Z} (W/Z \rightarrow q\bar{q}, p_T > 320, |\eta| < 1.9) = 8.5 \pm 0.8 \text{ (stat.)} \pm 1.5 \text{ (syst.) pb}$$

Consistent with NLO MCFM prediction within  $2\sigma$ :

$$\sigma_{W+Z}^{\text{MCFM}} = 5.1 \pm 0.5 \text{ pb}$$

## Systematics:

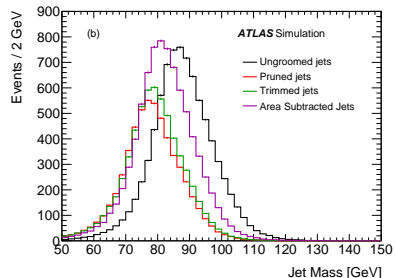
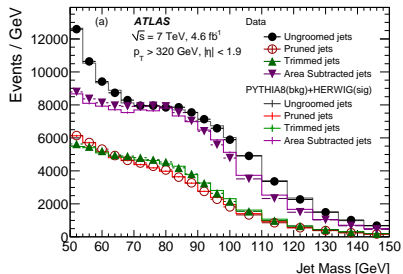
Sources	$\sigma_{W+Z}$
MC modelling	4.4 %
Background pdf	8.8 %
Signal pdf	5 %
Jet energy scale	3.7 %
Jet energy resolution	< 1 %
Jet mass scale	2.2 %
Jet mass resolution	12.6 %
$t\bar{t}$ contribution	2.8 %
Single-top and diboson contribution	< 1 %
$W$ and $Z$ relative yield	2.9 %
Luminosity	1.8 %
Total	18 %

# Effects of Various Grooming Techniques

18/20

- Use selected sample enriched in  $W/Z$  to study effect of
  - 1 pruning ( $R_{cut} = 0.3$ ,  $z_{cut} = 0.02$ ,  $k_t$ )
  - 2 trimming ( $R_{sub} = 0.2$ ,  $f_{cut} = 0.03$ )
  - 3 area subtraction

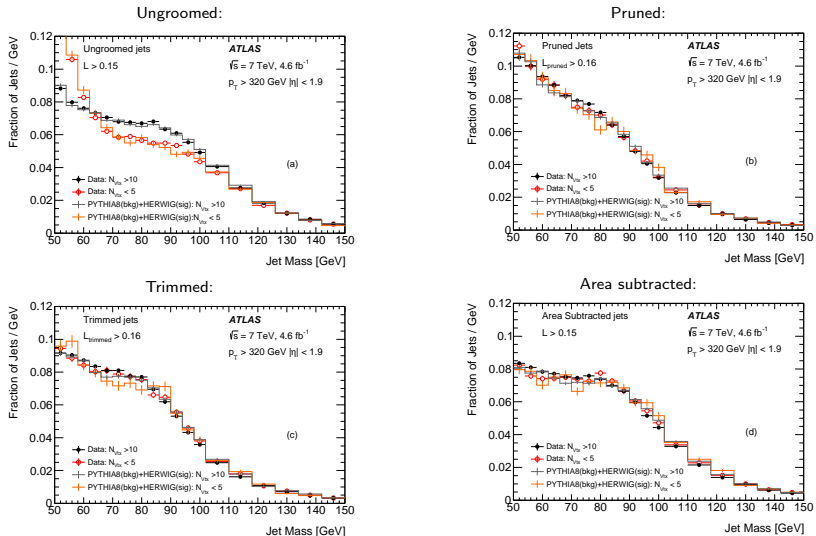
1 & 2 : cut on recalculated LLH to get the same background rejection (89%).  
3 : Recalculate area subtracted  $m_{jet}$  for default jets.



Without extra optimization, results are compatible with default analysis within statistical uncertainties.

# Low vs. High Pileup, i.e. $N_{Vtx} < 5$ vs. $N_{Vtx} > 10$

19/20



Pile-up is nicely suppressed, effect are well described by MC.

- New differential  $t\bar{t}$  cross section measurement @7 TeV
  - Comparison with MC generators, NLO(+NNLL) QCD computations and PDF sets
  - Data softer at high  $p_T^t$  than prediction, current reach: 900 GeV
- High  $p_T$  all-hadronic  $W/Z$  and  $Z \rightarrow b\bar{b}$  cross section measurements in good agreement with predictions
- Test of substructure techniques in events enriched with hadronically decaying  $W/Z$  shows good agreement with prediction and nice pile-up suppression.
- Looking forward to even more boosted Run-I/II measurements @ BOOST2015!

Backup

Backup

Backup

# $t\bar{t}$ Differential Cross Section – $\chi^2$ values

22/20

Variable	ALPGEN+HERWIG		MC@NLO+HERWIG		POWHEG+HERWIG		POWHEG+PYTHIA		NLO QCD		NLO+NNLL	
	$\chi^2/\text{NDF}$	$p\text{-value}$										
$p_T^t$	24./6	0.00	8.0/6	0.24	4.8/6	0.57	19./6	0.00	9.5/6	0.15	7.6/6	0.27
$m_{t\bar{t}}$	2.6/4	0.63	6.9/4	0.14	5.5/4	0.24	13./4	0.01	5.5/4	0.24	5.9/4	0.20
$p_T^{t\bar{t}}$	4.2/3	0.25	0.5/3	0.93	4.1/3	0.26	21./3	0.00	14./3	0.00	9.9/3	0.02
$ y_{t\bar{t}} $	1.6/2	0.45	3.4/2	0.18	4.3/2	0.11	4.8/2	0.09	3.7/2	0.16		

TABLE VII. Comparison between the measured normalized differential cross-sections and the predictions from several MC generators and theoretical calculations. For each variable and prediction a  $\chi^2$  and a  $p$ -value are calculated using the covariance matrix of each measured spectrum. The number of degrees of freedom (NDF) is equal to  $N_b - 1$  where  $N_b$  is the number of bins in the distribution. In the last column  $p_T^t$ ,  $m_{t\bar{t}}$  and  $p_T^{t\bar{t}}$  are compared to NLO+NNLL predictions [11] and [12–14].

Variable	CT10		MSTW2008NLO		NNPDF 2.3		HERAPDF 1.5	
	$\chi^2/\text{NDF}$	$p\text{-value}$	$\chi^2/\text{NDF}$	$p\text{-value}$	$\chi^2/\text{NDF}$	$p\text{-value}$	$\chi^2/\text{NDF}$	$p\text{-value}$
$p_T^t$	9.5/6	0.15	9.8/6	0.14	8.2/6	0.22	5.5/6	0.49
$m_{t\bar{t}}$	5.5/4	0.24	6.0/4	0.20	5.2/4	0.27	0.63/4	0.96
$p_T^{t\bar{t}}$	14./3	0.00	13./3	0.01	12./3	0.01	9.1/3	0.03
$ y_{t\bar{t}} $	3.7/2	0.16	4.0/2	0.13	1.3/2	0.52	0.44/2	0.80

TABLE VIII. Comparison between the measured normalized differential cross-sections and the NLO predictions (MCFM) for different parton distribution functions. For each kinematic variable and each parton distribution function, a  $\chi^2$  and a  $p$ -value are calculated using the covariance matrix of each measured spectrum as well as the theory PDF and scale covariance matrix. The number of degrees of freedom (NDF) is equal to  $N_b - 1$  where  $N_b$  is the number of bins in the distribution.

# $t\bar{t}$ Differential Cross Section – Systematic Uncertainties, Event Yields

23/20

$\frac{1}{\sigma} \frac{d\sigma}{dy_T}$  [Uncertainties %] / Bins [GeV]

	0-00	50-100	100-150	150-200	200-260	260-350	350-800
Jet energy scale	+0.2 -0.9	+1.0 -1.1	+1.0 -1.0	+2.4 -2.3	+2.1 -1.9	+2.5 -2.3	+3.6 -3.6
Jet energy resolution	+0.4 -0.4	+0.1 -0.5	— —	+0.3 -0.3	— —	+0.5 -0.5	— —
Jet reconstruction efficiency	— —	— —	— —	— —	— —	— —	+0.1 +0.1
b-quark tagging efficiency	+1.4 -1.4	+2.6 -2.6	+0.3 -0.3	+1.3 -1.3	+1.1 -1.1	+1.8 -1.8	+1.0 -1.0
c-quark tagging efficiency	— —	— —	— —	+0.1 -0.1	+0.1 -0.1	+0.2 -0.2	+0.2 -0.2
Light-jet tagging efficiency	+0.3 -0.3	— —	+0.2 -0.2	— —	— —	+0.2 -0.2	— —
Lepton selection and momentum scale	+1.8 -1.4	+1.7 -1.3	+1.2 -1.2	+0.6 -0.6	+0.9 -0.9	+1.1 -1.1	+1.0 -1.0
$E_T^{\text{miss}}$ unassociated cells	+0.4 -0.4	— —	+0.2 -0.2	— —	+0.3 -0.3	+0.3 -0.3	+0.3 -0.3
$E_T^{\text{miss}}$ pile-up	+0.8 -0.8	— —	+0.1 -0.1	+0.4 -0.4	+0.8 -0.8	+0.8 -0.8	+0.8 -0.8
MC generator	+1.8 -1.5	+2.6 -2.7	+0.2 -0.7	+1.3 -1.9	+0.1 -0.1	+3.5 -2.8	+15 -8.6
Fragmentation	+0.6 -0.6	+0.7 -0.7	— —	+0.8 -0.8	+0.9 -0.9	+0.7 -0.7	+1.0 -1.0
IFSR	+0.3 -0.3	+0.9 -0.9	— —	+3.2 -3.2	+1.2 -1.2	+1.8 -1.8	+1.0 -1.0
PDF	+0.1 -0.1	+0.1 -0.1	+0.2 -0.2	+0.5 -0.5	+0.8 -0.8	+0.8 -0.8	+0.8 -0.8
MC statistics	+1.0 -1.0	+0.4 -0.4	+0.7 -0.7	+0.9 -0.9	+1.1 -1.1	+1.4 -1.4	+2.6 -2.6
W+jets	+1.7 -1.7	+0.3 -0.3	+0.7 -0.7	+0.8 -0.8	+1.0 -1.0	+1.1 -1.1	+1.4 -1.4
Other backgrounds	+1.5 -1.5	+0.2 -0.2	+1.0 -1.0	+0.7 -0.7	+0.6 -0.6	+0.8 -0.8	+0.9 -0.9
Total systematic uncertainty	+5.3 -5.6	+1.8 -2.0	+2.7 -2.7	+4.8 -4.8	+4.9 -4.9	+5.3 -5.3	+12 -11

$\frac{1}{\sigma} \frac{d\sigma}{dy_T}$  [Uncertainties %]

	0.0-0.5	0.5-1.0	1.0-2.5
Jet energy scale	+0.6 -0.6	— —	+1.1 -0.9
Jet energy resolution	±0.1	±0.1	±0.4
Jet reconstruction efficiency	— —	— —	— —
b-quark tagging efficiency	— —	— —	— —
c-quark tagging efficiency	— —	— —	— —
Light-jet tagging efficiency	— —	— —	— —
Lepton selection and momentum scale	±0.4	±0.1	+0.9 -0.8
$E_T^{\text{miss}}$ unassociated cells	±0.1	— —	-0.2
$E_T^{\text{miss}}$ pile-up	— —	— —	0.1
MC generator	+2.5 -2.0	+4.1 -1.2	+5.0 -6.2
Fragmentation	+1.8 -1.9	+0.8 -0.8	+4.3 -4.1
IFSR	±0.1	— —	— —
PDF	±1.1	— —	+1.9 -2.0
MC statistics	±0.2	— —	±0.3
W+jets	±0.3	— —	+0.5 -0.4
Other backgrounds	±0.4	±0.1	±0.9
Total systematic uncertainty	+3.4 -3.1	+1.7 -1.5	+7.1 -7.9

$\frac{1}{\sigma} \frac{d\sigma}{dy_T}$  [Uncertainties [%] / Bins [GeV]]

	250-450	450-550	550-700	700-950	950-2700
--	---------	---------	---------	---------	----------

Jet energy scale	+1.4 -1.3	+0.8 -0.7	+2.1 -1.7	+3.0 -3.1	+3.6 -4.4
Jet energy resolution	±0.6	±0.9	±0.2	±0.2	—
Jet reconstruction efficiency	—	—	—	—	±0.2
b-quark tagging efficiency	+0.8 -1.0	±0.4 -1.3	+1.6 -1.3	+2.0 -1.3	+2.3 -1.7
c-quark tagging efficiency	— —	— —	±0.2 -0.2	— —	±0.1
Light-jet tagging efficiency	— —	±0.1 -0.1	— —	— —	±0.1
Lepton selection and momentum scale	±0.5	±0.8	±0.9	±1.7	+1.9 -1.8
$E_T^{\text{miss}}$ unassociated cells	— —	+0.1 -0.1	— —	— —	+0.5 -0.4
$E_T^{\text{miss}}$ pile-up	— —	-0.1 -0.1	+0.2 -0.2	+0.9 -0.9	+0.9 -0.9
MC generator	+2.7 -2.8	+1.9 -2.3	+2.6 -2.3	+3.0 -2.7	+2.5 -2.1
Fragmentation	±0.2	±0.2	+0.5 -0.5	+1.7 -1.7	+2.1 -2.1
IFSR	±0.5 -0.5	±0.2 -0.2	+0.9 -0.9	+1.4 -1.5	±0.4
PDF	— —	— —	— —	+0.5 -0.5	+2.2 -2.2
MC statistics	±0.4	±0.4	±0.6	±1.0	±1.6
W+jets	±0.2	+0.3 -0.3	+0.5 -0.4	+1.2 -1.0	+1.9 -1.7
Other backgrounds	±0.3	±0.7	+0.8 -0.8	+2.0 -2.0	+2.6 -2.4
Total systematic uncertainty	+3.4 -2.9	+2.6 -2.9	+4.1 -4.3	+6.1 -6.5	+8.0 -8.9

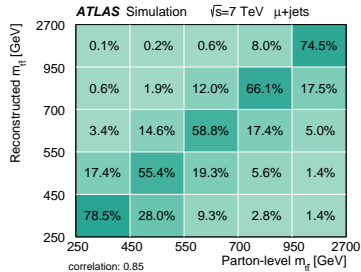
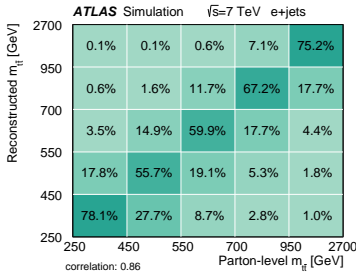
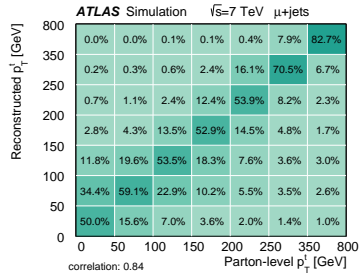
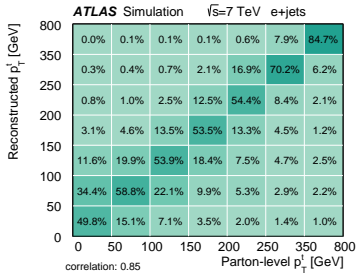
$e$ -jets       $\mu$ -jets

	$e$ -jets	$\mu$ -jets
$t\bar{t}$ ( $\ell+\text{jets}$ )	11200 ± 1500	13100 ± 1600
$t\bar{t}$ (dilepton)	850 ± 140	930 ± 140
Single top	560 ± 120	660 ± 150
$W+\text{jets}$	920 ± 240	1300 ± 300
Multijet	400 ± 200	200 ± 40
$Z+\text{jets}$	160 ± 70	89 ± 31
Diboson	22 ± 9	25 ± 9
Prediction	14100 ± 1600	16300 ± 1700
Data	13167	15752

TABLE II. Event yields in the  $e$ -jets and  $\mu$ -jets channels. The signal model, denoted  $t\bar{t}$  ( $\ell+\text{jets}$ ) in the table, is generated using ALPGEN. Errors indicate the total statistical and systematic uncertainties on each subsample and the uncertainty on the signal includes the generator systematic uncertainty discussed in Sec. IX B.

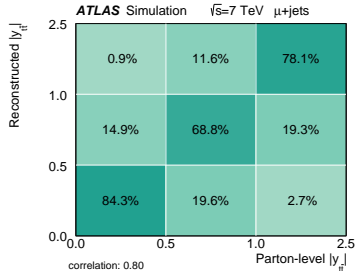
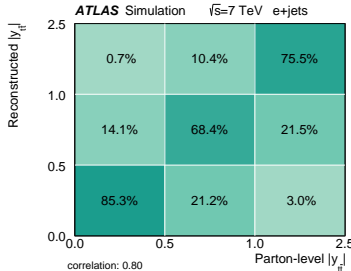
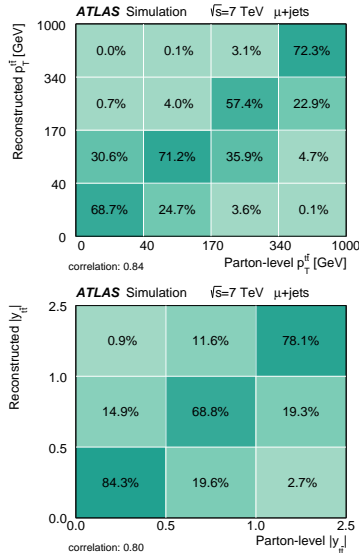
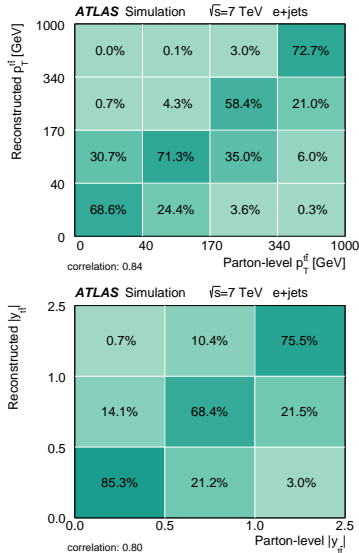
# $t\bar{t}$ Differential Cross Section – Migration Matrices I

24/20



# $t\bar{t}$ Differential Cross Section – Migration Matrices II

25/20



# $Z \rightarrow b\bar{b}$ : Details

## 5. Cross-section definition

The fiducial cross section of resonant  $Z$  boson production, with  $Z$  decaying to  $b\bar{b}$ ,  $\sigma_{Z \rightarrow b\bar{b}}^{\text{fid}}$ , is defined as follows. Particle-level jets in MC  $Z \rightarrow b\bar{b}$  events are reconstructed from stable particles (particles with lifetime in excess of 10 ps, excluding muons and neutrinos) using the anti- $k_t$  algorithm with radius parameter  $R = 0.4$ . There must be two particle-level  $b$ -jets in the event that satisfy the following fiducial conditions:  $p_T > 40 \text{ GeV}$ ,  $|\eta| < 2.5$  for the individual jets; and  $\Delta R(\text{jet1}, \text{jet2}) < 1.2$ ,  $p_T^{\text{dijet}} > 200 \text{ GeV}$ ,  $60 < m_{\text{dijet}} < 160 \text{ GeV}$  for the dijet system.

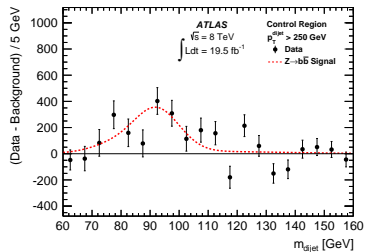
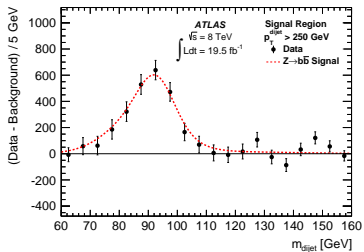
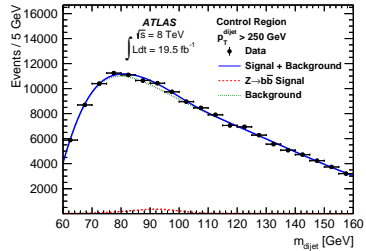
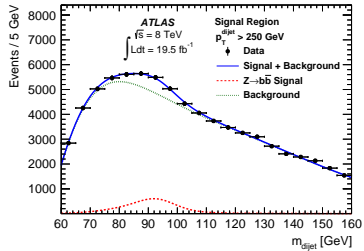
The cross section is extracted from the measured yield of  $Z \rightarrow b\bar{b}$  events in the data,  $N_{Z \rightarrow b\bar{b}}$ , as

$$\sigma_{Z \rightarrow b\bar{b}}^{\text{fid}} = \frac{N_{Z \rightarrow b\bar{b}}}{\mathcal{L} \cdot C_{Z \rightarrow b\bar{b}}},$$

where  $C_{Z \rightarrow b\bar{b}}$  is the efficiency correction factor to correct the detector-level  $Z \rightarrow b\bar{b}$  yield to the particle level. The value of  $C_{Z \rightarrow b\bar{b}}$  in the SHERPA MC signal is found to be 16.2%, which can be factorised into the product of: trigger efficiency (88.1%),  $b$ -tagging and kinematic selection efficiency (52.7%), and the efficiency of the  $S_{NN}$  requirement that defines the Signal Region (35.0%).

Source of uncertainty	$\Delta N_{Z \rightarrow b\bar{b}}(\%)$	$\Delta C_{Z \rightarrow b\bar{b}}(\%)$	$\Delta \sigma_{Z \rightarrow b\bar{b}}^{\text{fid}}(\%)$
Jet energy scale	+3.0 / -1.5	$\pm 8.4$	+6.5 / -5.0
Jet energy resolution	$\pm 5.3$	$\pm 0.2$	$\pm 5.1$
$b$ -tagging	$\pm 0.1$	$\pm 3.6$	$\pm 3.6$
Trigger modelling	N/A	$\pm 6$	$\pm 6$
Control Region bias	+4.9 / -5.5	N/A	+4.9 / -5.5
Signal $S_{NN}$ modelling	$\pm 0.9$	$\mp 2.0$	$\pm 2.9$
Signal $m_{\text{dijet}}$ shape	$\pm 2.2$	N/A	$\pm 2.2$
$Z \rightarrow c\bar{c}$ normalisation	$\pm 0.4$	N/A	$\pm 0.4$
$t\bar{t}$ normalisation	$\pm 1.2$	N/A	$\pm 1.1$
$W \rightarrow q\bar{q}'$ normalisation	$\pm 1.0$	N/A	$\pm 1.0$

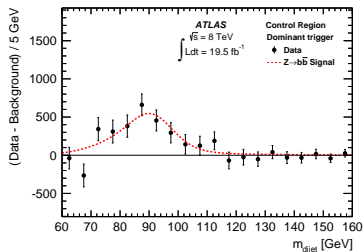
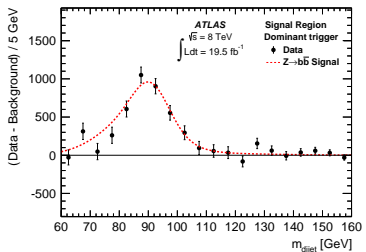
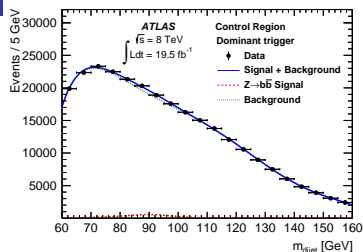
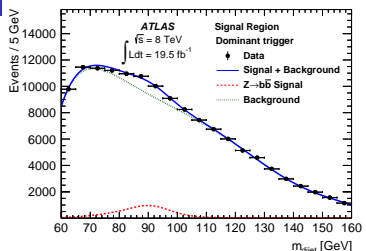
# Fit Validation, $p_T^{dijet}$ raised from 200 to 250 GeV



This yield measurement, extrapolated back to the baseline fiducial cross-section definition (i.e. with dijet  $p_T > 200 \text{ GeV}$ ), results in a consistent cross section of  $2.11 \pm 0.28 \text{ (stat.) pb}$ .

# Fit Validation, only events selected by the dominant trigger

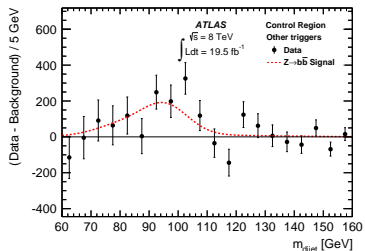
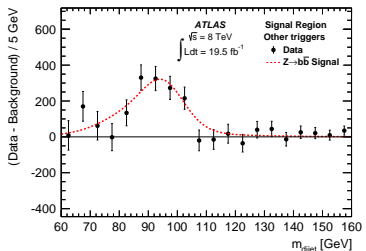
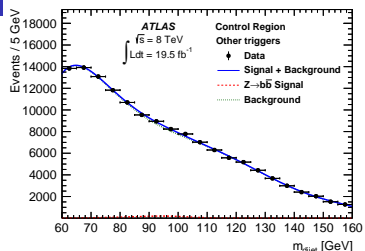
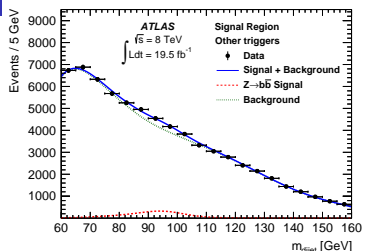
28/20



Statistically independent compared to next page, compatible results:  $1.99 \pm 0.25 \text{ (stat.) pb}$  and  $1.87 \pm 0.44 \text{ (stat.) pb}$  respectively, despite the very different background shapes that are produced by the different kinematic sculpting effects of the triggers and the conservative trigger modelling systematic uncertainty of the measurement.

# Fit Validation, only events NOT selected by the dominant trigger

29/20



Statistically independent compared to last page, compatible results:  $1.87 +/- 0.44 \text{ (stat.) pb}$  and  $1.99 +/- 0.25 \text{ (stat.) pb}$  respectively, despite the very different background shapes that are produced by the different kinematic sculpting effects of the triggers and the conservative trigger modelling systematic uncertainty of the measurement.

# W/Z: Event Shape Variables

30/20

- Thrust minor: the thrust axis [34, 35] of a jet in its centre-of-mass frame,  $\hat{T}$ , is defined as the direction which maximizes the sum of the longitudinal momenta of the energy clusters. The thrust minor [34, 35],  $T_{\min}$ , is related to this direction and is defined as

$$T_{\min} = \frac{\sum_i |\vec{p}_i \times \hat{T}|}{\sum_i |\vec{p}_i|}, \quad (\text{A.1})$$

where  $\vec{p}_i$  are the momenta of the energy clusters in the jet rest frame.  $T_{\min} = 0$  corresponds to a highly directional distribution of the energy clusters, and  $T_{\min} = 0.5$  corresponds to an isotropic distribution.

- Sphericity: the sphericity tensor [36] is defined as

$$S^{\alpha\beta} = \frac{\sum_i p_i^\alpha p_i^\beta}{\sum_i |\vec{p}_i|^2}, \quad (\text{A.2})$$

where  $\alpha$  and  $\beta$  correspond to the  $x$ ,  $y$  and  $z$  components of the momenta of the energy clusters in the jet rest frame. By standard diagonalization of  $S^{\alpha\beta}$  one may find three eigenvalues  $\lambda_1 \geq \lambda_2 \geq \lambda_3$ , with  $\lambda_1 + \lambda_2 + \lambda_3 = 1$ . The sphericity is then defined as

$$S = \frac{3}{2}(\lambda_2 + \lambda_3). \quad (\text{A.3})$$

Sphericity is a measure of the summed squares of transverse momenta of all the energy clusters with respect to the jet axis. By construction  $0 \leq S \leq 1$ . A jet with two back-to-back subjets in its rest frame has  $S = 0$ , and  $S = 1$  indicates an isotropic distribution of the energy clusters.

- Aplanarity: the aplanarity [36] is defined as

$$A = \frac{3\lambda_3}{2}, \quad (\text{A.4})$$

and is constrained to the range  $0 \leq A \leq \frac{1}{2}$ . A highly directional distribution of the energy clusters has  $A = 0$ , and  $A = 0.5$  corresponds to an isotropic distribution.

[34] S. Brandt, Ch. Peyrou, R. Sosnowski, and A. Wroblewski, *The principal axis of jets — an attempt to analyze high-energy collisions as two-body processes*, Phys. Lett. **12** (1964) 57.  
 [35] E. Farhi, *Quantum Chromodynamics Test for Jets*, Phys. Rev. Lett. **39** (1977) 1587.  
 [36] J. D. Bjorken and S. J. Brodsky, *Statistical Model for Electron-Positron Annihilation Into Hadrons*, Phys. Rev. **D1** (1970) 1416.